Darcy flow in a wavy channel filled with a porous medium

Donald D. Gray

National Energy Technology Laboratory, Morgantown, WV 26507-0880

Department of Civil & Environmental Engineering, West Virginia University, Morgantown, WV 26506-6103

304-293-9933

304-293-7109 (fax)

gray@cemr.wvu.edu

Egemen Ogretim

National Energy Technology Laboratory, Morgantown, WV 26507-0880

Department of Civil & Environmental Engineering, West Virginia University, Morgantown, WV 26506-6103

Egemen.ogretim@gediz.edu.tr

Grant S. Bromhal

National Energy Technology Laboratory, Morgantown, WV 26507-0880

304-285-4688

Bromhal@netl.doe.gov

Abstract Flow in channels bounded by wavy or corrugated walls is of interest in both technological and geological contexts. This paper presents an analytical solution for the steady Darcy flow of an incompressible fluid through a homogeneous, isotropic porous medium filling a channel bounded by symmetric wavy walls. This packed channel may represent an idealized packed fracture, a situation which is of interest as a potential pathway for the leakage of carbon dioxide from a geological sequestration site. The channel walls change from parallel planes, to small amplitude sine waves, to large amplitude nonsinusoidal waves as certain parameters are increased. The direction of gravity is arbitrary. A plot of piezometric head against distance in the direction of mean flow changes from a straight line for parallel planes to a series of steeply sloping sections in the reaches of small aperture alternating with nearly constant sections in the large aperture bulges. Expressions are given for the stream function, specific discharge, piezometric head, and pressure.

Keywords *Wavy channel, Porous media, Darcy's law, flow in a fracture*

1 Introduction

Flow in channels bounded by wavy or corrugated walls is of interest in both technological and geological contexts. In some cases, the channel is occupied entirely by the flowing fluid (this is called an unpacked channel). In other cases it is filled by a saturated porous medium (this is called a packed channel). Heat exchangers, membrane blood oxygenators, filters, and chemical reactors are typical engineered applications of channel flow. In hydrogeology, geotechnical engineering, and petroleum engineering the flow of groundwater or hydrocarbons through fractures is of fundamental importance. The direct motivation for this paper is the potential role of packed fractures as pathways for the leakage of carbon dioxide from geological sequestration sites.

Flow through channels has attracted the attention of numerous investigators. Huitt (1956) performed laboratory experiments to measure friction factors for laminar and turbulent flow in unpacked channels bounded by smooth and sand-roughened parallel planes. For sand-packed channels he found that the Ergun equation, which relates the friction factor to porosity and particle diameter, gave adequate predictions.

Chow et al. (1971) used second order perturbation analysis to solve for the incompressible viscous flow in an unpacked symmetric channel with small amplitude sinusoidal walls.

Nishimura et al. (1984) performed laboratory experiments in an unpacked channel with large amplitude sinusoidal wavy walls covering the range of Reynolds numbers (*Re*) from about 40 to 10 000. They measured the wall shear stress and used the hydrogen bubble technique to observe the flow pattern. They also used a finite element code to predict the streamlines from $Re = 1$ to 700. The streamline pattern was symmetric and showed no evidence of separation for $Re < 15$. They found good agreement between experiment and computation for $Re < 350$ when unsteady motion was first observed in the experiment. The flow became turbulent at higher *Re*.

Datta and Tripathi (2010) studied viscous flow in an unpacked antisymmetric channel whose walls were small amplitude sine waves. They used a non-orthogonal coordinate system to obtain a first order perturbation solution.

In the hydrogeology literature, the link between laminar viscous flow in an unpacked channel and Darcy flow in a fractured porous medium is attributed to Romm (1966). By rewriting the Poiseuille solution for viscous flow between parallel planes in the form of Darcy's law, he showed that the equivalent hydraulic conductivity $K'$is proportional to the square of the aperture a'

$$K' = \frac{\rho' g' a'^2}{12\mu'}$$

where ρ' is the fluid density, g' is the acceleration due to gravity, and μ' is the dynamic viscosity. (Note that primes are used throughout this paper to indicate dimensional quantities.) Using this formula for conductivity in Darcy's law, the volumetric flowrate $Q'$is found to be proportional to a'^3. This result is referred to as the "cubic law" and is the basis for many analyses of flow in fractured rock formations (Domenico and Schwartz, 1998).

Zimmerman and Bodvarsson (1996) reviewed the cubic law and its extension to flow in unpacked channels bounded by rough walls. They carefully elucidated the range of conditions under which the Navier-Stokes equations can be approximated by the Reynolds lubrication equations or the Hele-Shaw equations. They treated the effect of actual contact between the bounding walls by using the Hele-Shaw model.

As measurement techniques have improved in recent years, several authors have measured fractures with complex geometries (Hughes and Blunt, 2001; Konzuk and Kueper, 2004; Piri and Karpyn, 2007). Crandall et al. (2010) used computational fluid dynamics modeling of flow through a rough walled fracture with a geometry derived from x-ray computed tomography (CT) images of a fracture in a sandstone core to investigate the deviation from the cubic law as a function of fracture aperture.

Ng and Wang (2010) studied steady flow in channels bounded by walls whose corrugations were small amplitude sine waves. The resistance to flow was modeled by the Darcy-Brinkman equation which contains terms for both creeping viscous flow and Darcian porous media flow. Second order perturbation analysis

was used to obtain solutions for flow parallel to the corrugations (longitudinal flow) and flow normal to the corrugations (cross flow). Wavelength, phase difference, and permeability effects were explored.

2 Problem statement and solution

Consider a channel bounded by an impermeable wavy surface and its reflection across a center plane. The generators of the wavy surfaces are straight lines parallel to each other and to the center plane. The waves are periodic with wavelength λ', but are not necessarily sinusoidal. Figure 1 shows a one-cycle length of the channel and an orthogonal coordinate system with the origin in the plane of symmetry. The y' axis is parallel to the generators of the wavy surfaces, and the z'axis is normal to the plane. The channel extends indefinitely in the x' and y' directions, and in this study there is no flow in the y' direction because the piezometric head does not vary with y'. The bounding wavy surfaces pass through $(x' = 0, y', z' = \pm L')$. The direction of the gravity vector is arbitrary.

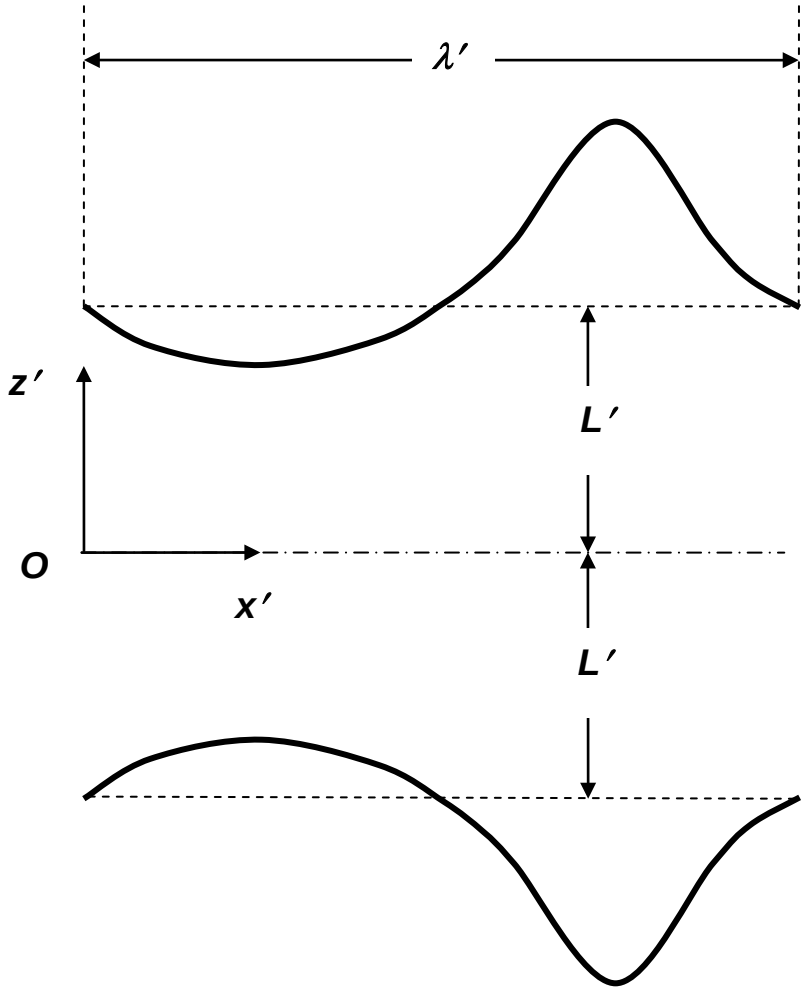

Fig. 1 Geometric definition sketch. Heavy lines show one cycle of the periodic surfaces. The surfaces extend without change in the y' direction (normal to the page), x' is the direction of mean flow, and z' is transverse to the gap. The direction of the gravity vector is arbitrary.

The channel, which may represent an idealized geologic packed fracture, is filled with a saturated, homogeneous, isotropic porous medium whose hydraulic

conductivity is K'. To be more precise, the porous medium considered here is what Auriault (2009) calls a classical porous medium: a connected solid structure whose pore space depends on the characteristic pore size. Auriault shows that for a porous medium of this type, "The flow is governed by Darcy's law".

The continuity equation for the steady two dimensional motion of an incompressible fluid through a static porous medium is

$$\frac{\partial u'}{\partial x'} + \frac{\partial w'}{\partial z'} = 0 \tag{1}$$

where u' is the specific discharge (Darcy velocity) in the x' direction and w' is the specific discharge in the z' direction. For Reynolds numbers less than about 1 (based on the specific discharge and an average grain diameter), the momentum balance is accurately modeled by the x' and z' components of Darcy's law (Bear 1972):

$$u' = -K' \frac{\partial h'}{\partial x'} \tag{2}$$

$$w' = -K' \frac{\partial h'}{\partial z'} \tag{3}$$

Here h' is the piezometric head given by

$$h' = \frac{p'}{\rho' g'} + \zeta' \tag{4}$$

where p' is the pressure, and ζ' is the elevation (measured positive upward). The elevation of a point is related to its coordinates by

$$\zeta' = x' \cos(\zeta', x') + y' \cos(\zeta', y') + z' \cos(\zeta', z') + \zeta'_0 \tag{5}$$

where $\cos(\zeta', x')$ is the cosine of the angle between the positive ζ' and x' directions, etc., and ζ'_0 is the elevation of the origin.

The problem is transformed to dimensionless (unprimed) variables using the following definitions.

$$\begin{aligned} &x' = \lambda' x, \quad && y' = \lambda' y, \quad && z' = \lambda' z, \\ &\zeta' = \lambda' \zeta, \quad && h' = \lambda' h, \quad && L' = \lambda' L \\ &u' = U' u, \quad && w = U' w, \quad && K' = U' K \\ &\rho' = \rho' \cdot \rho, \quad && && g' = (U'^2/\lambda') g \end{aligned} \tag{6}$$

The dimensionless wavelength becomes 1, and U' is a characteristic value of the specific discharge. The dimensionless equations can be obtained formally simply by omitting the primes in Equations 1-5.

Equation 1 is identically satisfied by the dimensionless stream function ψ whose derivatives are related to the dimensionless specific discharge by

$$u = \frac{\partial \psi}{\partial z} \tag{7}$$

$$w = -\frac{\partial \psi}{\partial x} \tag{8}$$

As demonstrated by Bear (1972), a flow governed by Equations 1-3 is irrotational. Substitution of Equations 7 and 8 into the condition of irrotationality shows that ψ obeys the Laplace equation. The linearity of the Laplace equation permits the use of the principle of superposition to solve for the stream function as the sum of a term corresponding to a uniform flow in the *x* direction and a term that depends on the wall shape. This solution, which has been obtained by the method of separation of variables, is

$$\psi(x,z) = z + \frac{\mathcal{V}\sin(2\pi x)\sinh(2\pi z)}{2\pi\sinh(2\pi L)} \tag{9}$$

where $\mathcal{V}$ is a dimensionless constant related to the amplitude of the walls. Each streamline corresponds to a fixed value of ψ. In particular, the centerplane is given by $\psi = 0$, and the upper and lower wall contours $z_{s\pm}$ are given by

$$\psi(x, z_{s\pm}) = \pm L \tag{10}$$

The coordinates of any streamline can be determined by fixing a value of ψ, where $-L \leq \psi \leq L$, and solving Equation 9 iteratively for *z* as *x* is scanned through the desired range. Because the no slip condition does not hold for the specific discharge, any pair of streamlines can be interpreted as the impermeable boundaries of a channel.

Differentiating Equation 9 as prescribed by Equations 7 and 8, the components of the specific discharge are found to be

$$u = 1 + \frac{\mathcal{V}\sin(2\pi x)\cosh(2\pi z)}{\sinh(2\pi L)} \tag{11}$$

$$w = -\frac{\mathcal{V}\cos(2\pi x)\sinh(2\pi z)}{\sinh(2\pi L)} \tag{12}$$

From Equation 12 it can be deduced that $\mathcal{V} = w(0, -L)$.

The dimensionless flowrate Q is found by integrating u over the dimensionless channel cross section.

$$Q = \int_A udA = b \int_{z_{s-}}^{z_{s+}} udz = 2b \int_0^{z_{s+}} udz$$

where b is the dimensionless breadth of the channel, i.e. in the y direction. Substituting Equation 11 for u and integrating gives.

$$\frac{Q}{2b} = \int_0^{z_{s+}} \left[1 + \frac{\mathcal{V} sin(2\pi x) cosh(2\pi z)}{sinh(2\pi L)}\right] dz$$

$$= [z_{s+} - 0] + \mathcal{V} \frac{sin(2\pi x)}{2\pi\, sinh(2\pi L)} [sinh(2\pi z_{s+}) - sinh(0)]$$

Replacing z_{s+} from Equation 9

$$\frac{Q}{2b} = \left[L - \mathcal{V} \frac{sin(2\pi x)\, sinh(2\pi z_{s+})}{2\pi\, sinh(2\pi L)}\right] + \mathcal{V} \frac{sin(2\pi x)\, sinh(2\pi z_{s+})}{2\pi\, sinh(2\pi L)}$$

leads to the simple result that

$$Q = 2bL \tag{13}$$

Dividing Q/b by the dimensionless channel aperture, $2z_{s+}$, gives the dimensionless average specific discharge $\overline{u}$ in the x direction.

$$\overline{u(x)} = \frac{L}{\left[L - \frac{\mathcal{V} \sin(2\pi x) \sinh(2\pi z_{s+})}{2\pi \sinh(2\pi L)}\right]} \tag{14}$$

Substitution of Equations 11 and 12 into the dimensionless forms of Equations 2 and 3, followed by partial integration enables the determination of the dimensionless piezometric head distribution.

$$h(x, z) = h(0,0) - \frac{x}{K} + \frac{\mathcal{V}[\cos(2\pi x) \cosh(2\pi z) - 1]}{2\pi K \sinh(2\pi L)} \tag{15}$$

where it is assumed that the dimensionless head at the origin is known. The corresponding dimensionless pressure distribution is given by

$$p(x,z) = p(0,0) - \rho g[x\cos(\zeta,x) + y\cos(\zeta,y) + z\cos(\zeta,z)] - \frac{\rho g x}{K} + \frac{\rho g \mathcal{V}[\cos(2\pi x)\cosh(2\pi z) - 1]}{2\pi K \sinh(2\pi L)} \quad (16)$$

3 Results

The dimensionless width parameter L and the dimensionless amplitude parameter $\mathcal{V}$ determine the shape of the flow passage. Inspection of Equation 9 shows that the boundaries reduce to parallel planes for $\mathcal{V} = 0$. This corresponds to uniform parallel flow in the x direction and a constant rate of head loss in the x direction. The value of $\mathcal{V}$ is bounded because the x component of the specific discharge cannot become negative. It appears that there is no exact closed form expression for this limit, but for small L it is very closely approximated by

$$\mathcal{V} < \tanh(2\pi L) \quad (17)$$

For large values of L the upper limit is considerably less than $\tanh(2\pi L)$. Values of $\mathcal{V}$ which exceed the limit cause divergence of the solution for z_{s+}.

Figure 2 shows that for fixed L, the walls are small amplitude sine waves when $\mathcal{V}$ is small, but become increasingly nonsinusoidal as $\mathcal{V}$ increases. For large $\mathcal{V}$ the form of the channel approaches a series of long thin fissures separated by short bulging chambers.

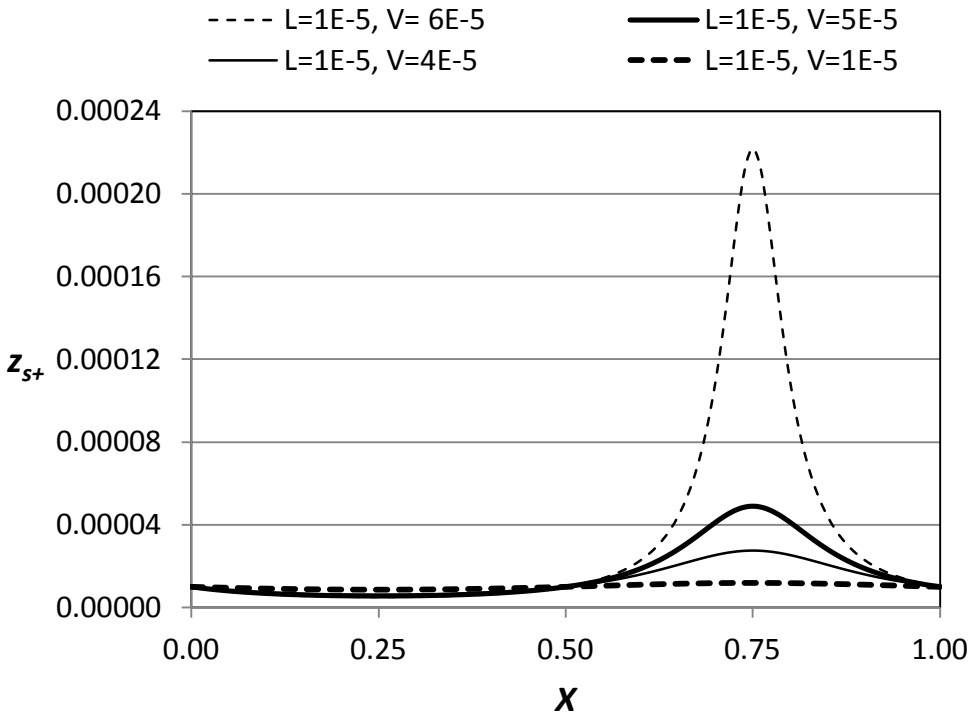

Fig. 2 Upper bounding surface shapes for $L = 1\ \mathrm{E} - 5$ and $\mathcal{V} = 1\ \mathrm{E} - 5$ to $6\ \mathrm{E} - 5$.

Figure 3 shows that the effect of increasing L with $\mathcal{V}$ fixed is to increase the aperture of the channel and also to reduce the deviation from a sinusoidal shape.

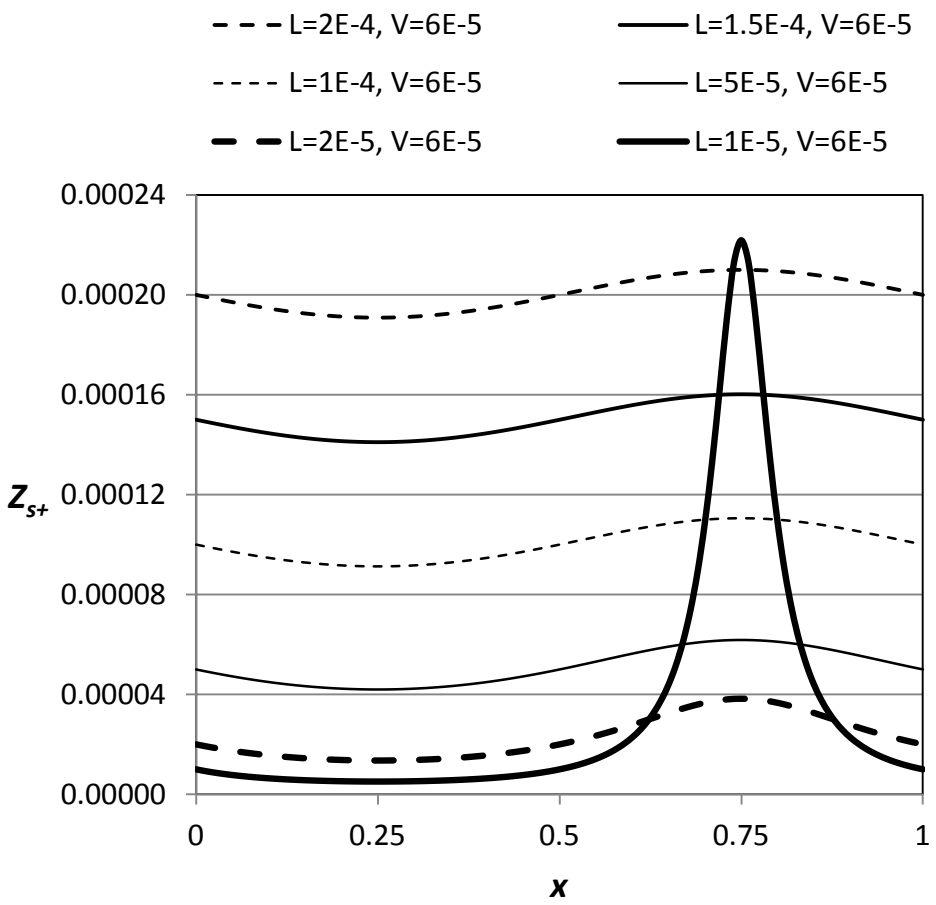

Fig. 3 Upper bounding surface shapes for $L = 1\ \mathrm{E}-5$ to $2\ \mathrm{E}-4$ and $\mathcal{V} = 6\ \mathrm{E}-5$.

Figures 4 and 5 show the streamline patterns for different values of L and $\mathcal{V}$. Increasing $\mathcal{V}$ from 3 E-5 to 6 E-5 and increasing L from 1 E-3 to 1 E-5 greatly magnifies the difference between the largest and smallest apertures while increasing the proportion of the channel occupied by the small aperture regions.

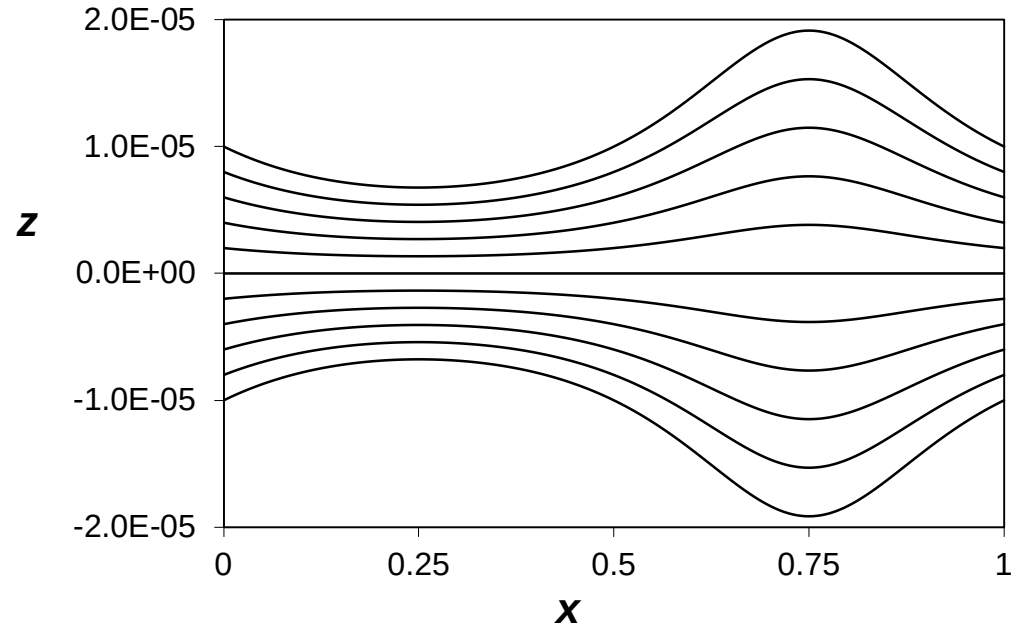

Fig. 4 Dimensionless streamlines for flow between wavy surfaces for $\mathcal{V} = 3\ \mathrm{E} - 5, L = 1\ \mathrm{E} - 5$.

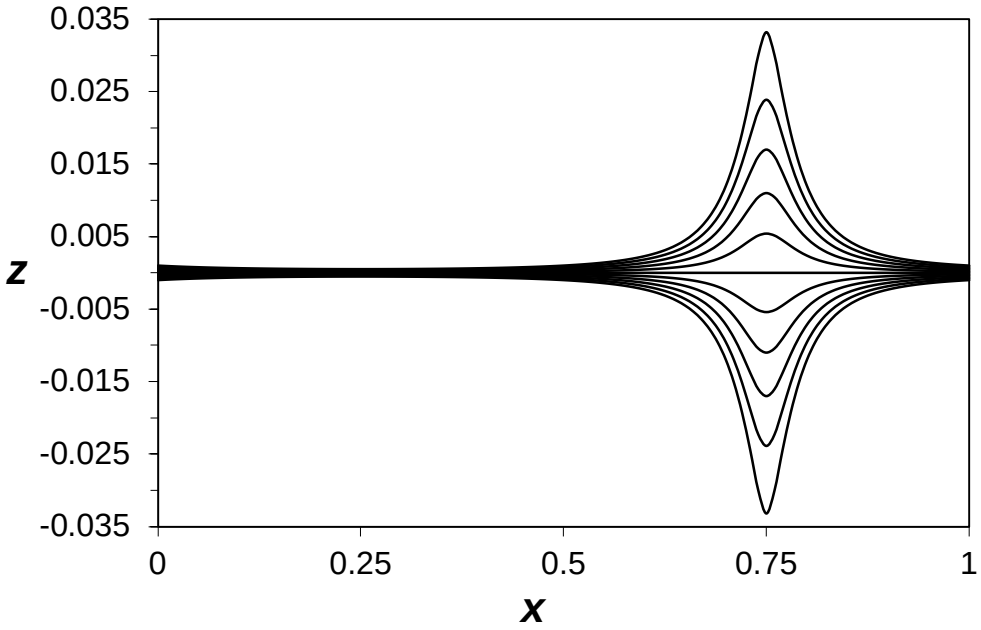

Fig. 5 Dimensionless streamlines for flow between wavy surfaces for $\mathcal{V} = 6\,\mathrm{E}-5, L = 1\,\mathrm{E}-3$.

Figures 6 and 7 show the variation in centerplane dimensionless piezometric head and dimensionless specific discharge with *x* for the same cases as Figures 4 and 5, respectively. As seen from Equation 15, the head depends also on the dimensionless hydraulic conductivity and the head at the origin, which have the same values in these two figures. As expected, the centerline specific discharge goes through a much wider excursion in the more extreme channel. In both cases, the head drops in a noticeably nonlinear fashion, but the deviation is far more pronounced in the more extreme channel. The head drops more rapidly in the narrow aperture reaches where the specific discharge is greater and much less steeply through the chambers.

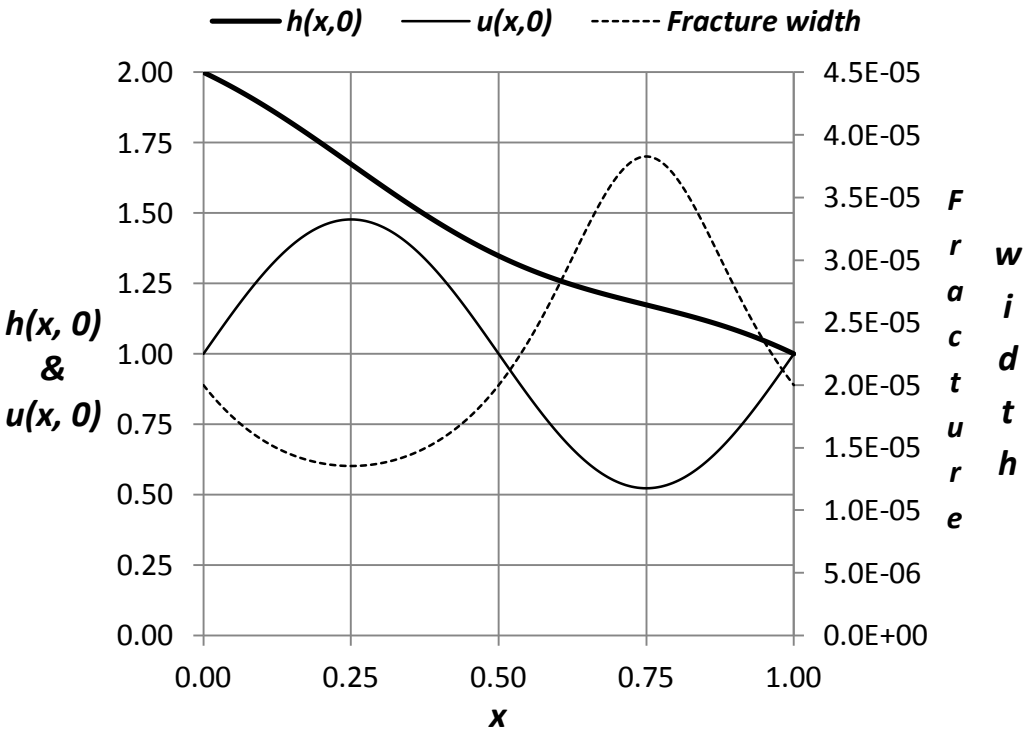

Fig. 6 Dimensionless centerplane head, centerplane specific discharge, and aperture for $\mathcal{V} = 3\ \mathrm{E} - 5, L = 1\ \mathrm{E} - 5, K = 1, h(0{,}0) = 2$.

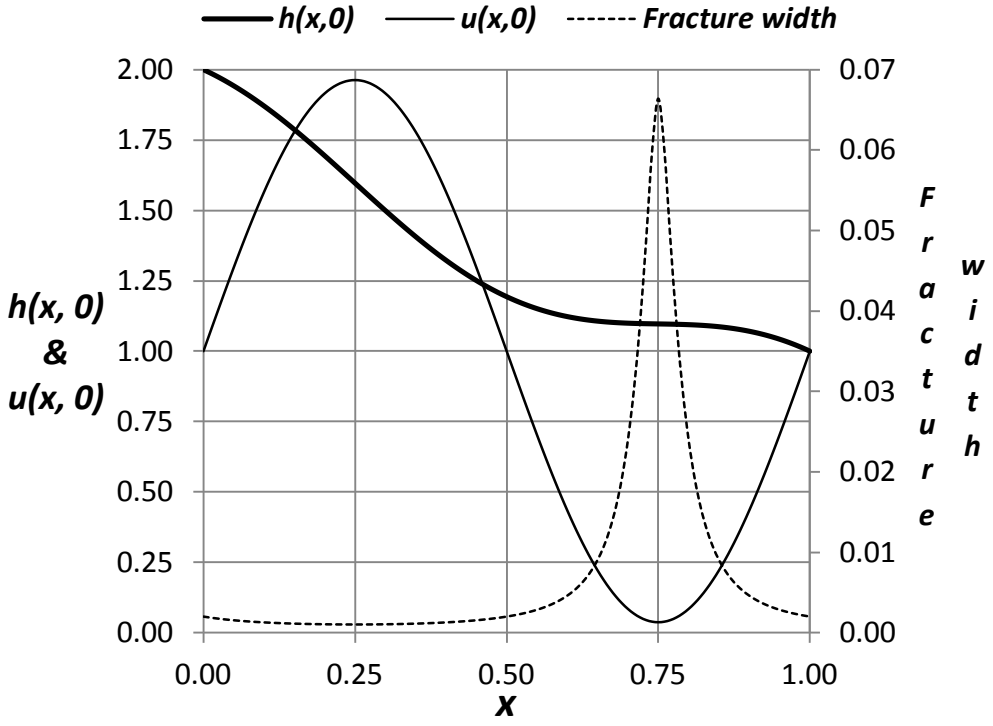

Fig. 7 Dimensionless centerplane head, centerplane specific discharge, and fracture width for $\mathcal{V} = 6\ \mathrm{E} - 5, L = 1\ \mathrm{E} - 3, K = 1, h(0{,}0) = 2$.

Figure 8 shows that for a fixed value of L, increasing $\mathcal{V}$ escalates the amplitude of the specific discharge averaged over the cross section of the channel. When $\mathcal{V}$ is held constant, increasing L decreases the amplitude of $\overline{u}$ as illustrated in Figure 9.

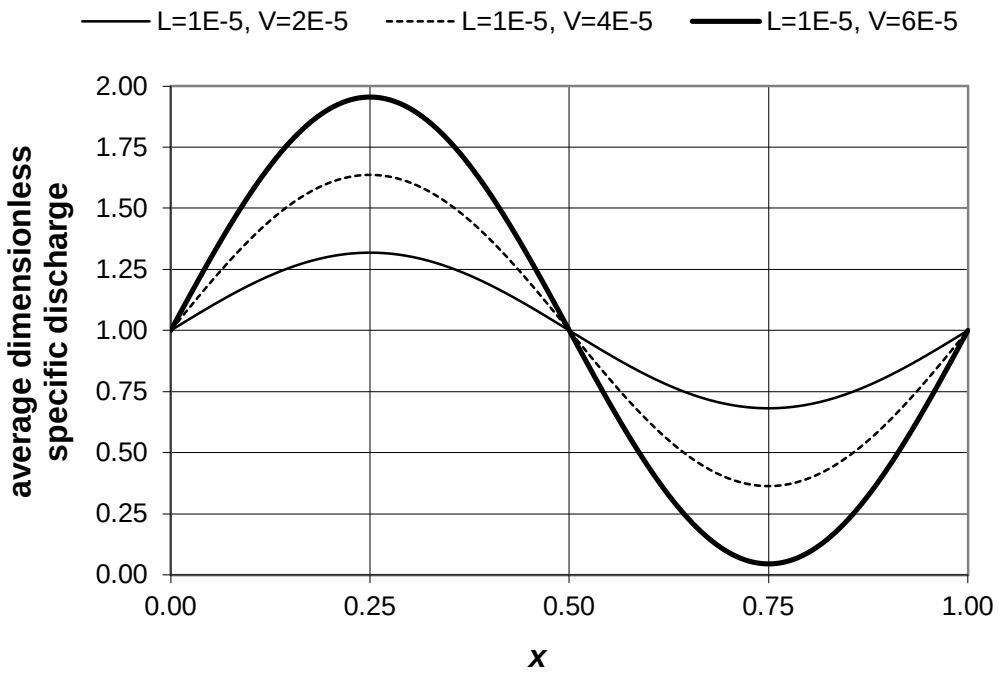

Fig. 8 Average dimensionless specific discharge $\overline{u(x)}$ for $L = 1\ \mathrm{E}-5$ and $\mathcal{V} = 2\ \mathrm{E}-5$ to $6\ \mathrm{E}-5$.

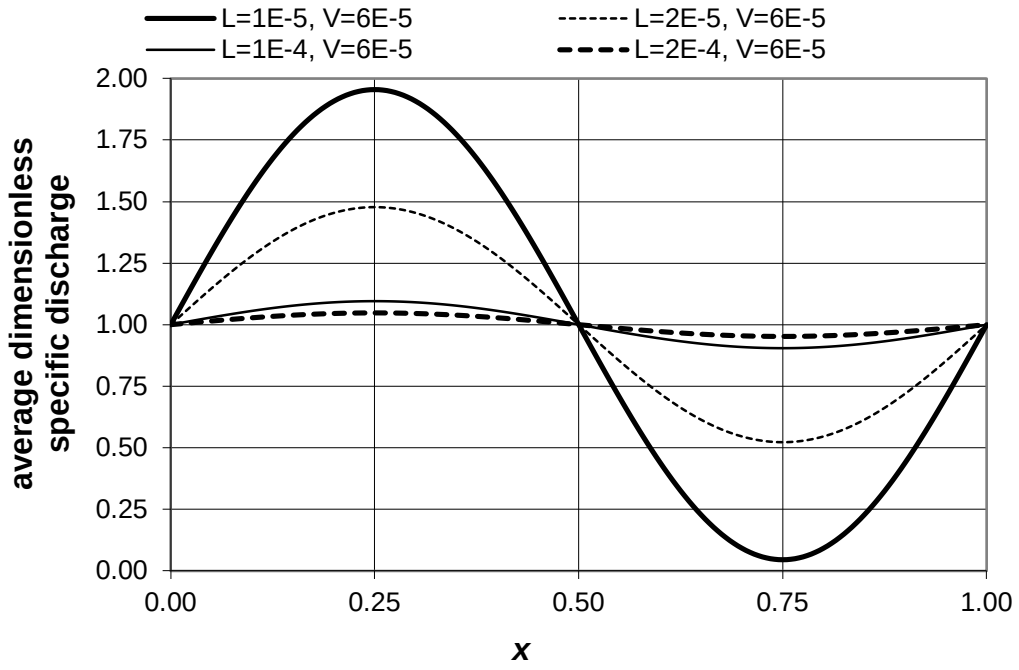

Fig. 9 Average dimensionless specific discharge $\overline{u(x)}$ for $L = 1\text{ E} - 5$ to $2\text{ E} - 4$ and $\mathcal{V} = 6\text{ E} - 5$.

The variation of *u* with *z* at various values of *x* is depicted in Figures 10 and 11. In Figure 10, $0 \leq x \leq 0.5$, which corresponds to an aperture $\leq 2L$. Here the specific discharge is uniform at $x = 0$ and increases with distance from the centerplane to an increasing degree until $x = 0.25$. Beyond $x = 0.25$, the profile flattens until it is again uniform at $x = 0.5$. Figure 11 covers the range of $0.5 \leq x \leq 1$, for which the aperture $\geq 2L$. It shows how *u* decreases away from the centerplane to an increasing degree until $x = 0.75$ and then flattens until it is again uniform at $x = 1$. Separate plots have been used for the two halves of the cycle because the amplitudes of *u* and *z* differ greatly for the case shown.

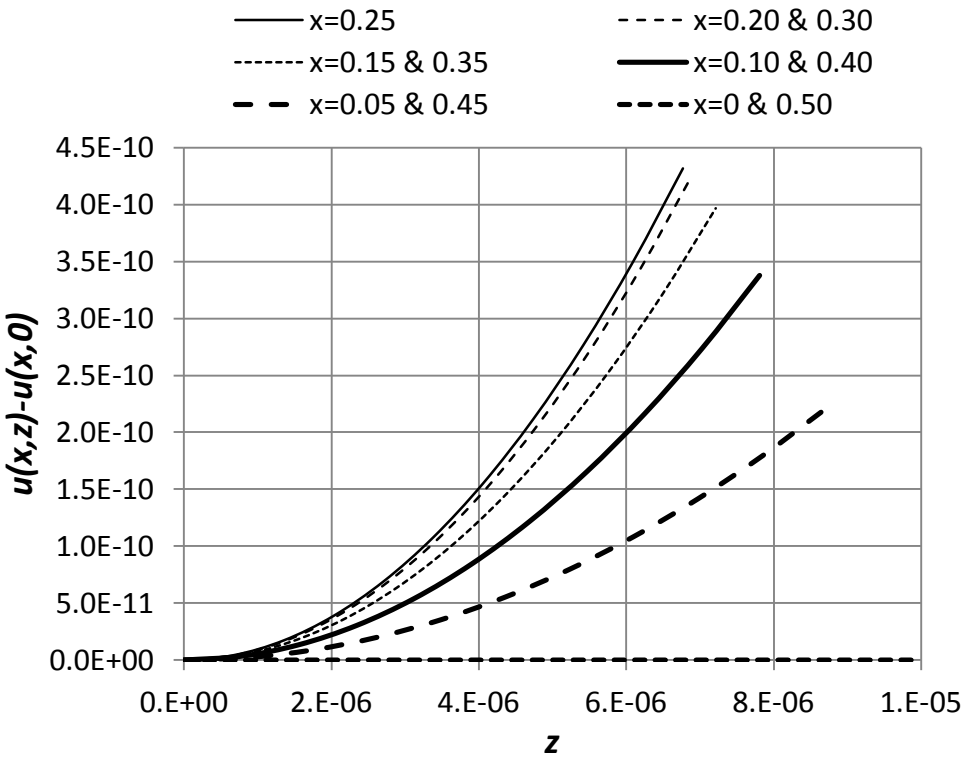

Fig 10 *u(x, z)-u(x, 0)* for x = 0, 0.05, 0.10, 0.15, 0.20, 0.25, 0.30, 0.35, 0.40, 0.45, 0.50, with L = 1 E - 5, V = 3 E - 5

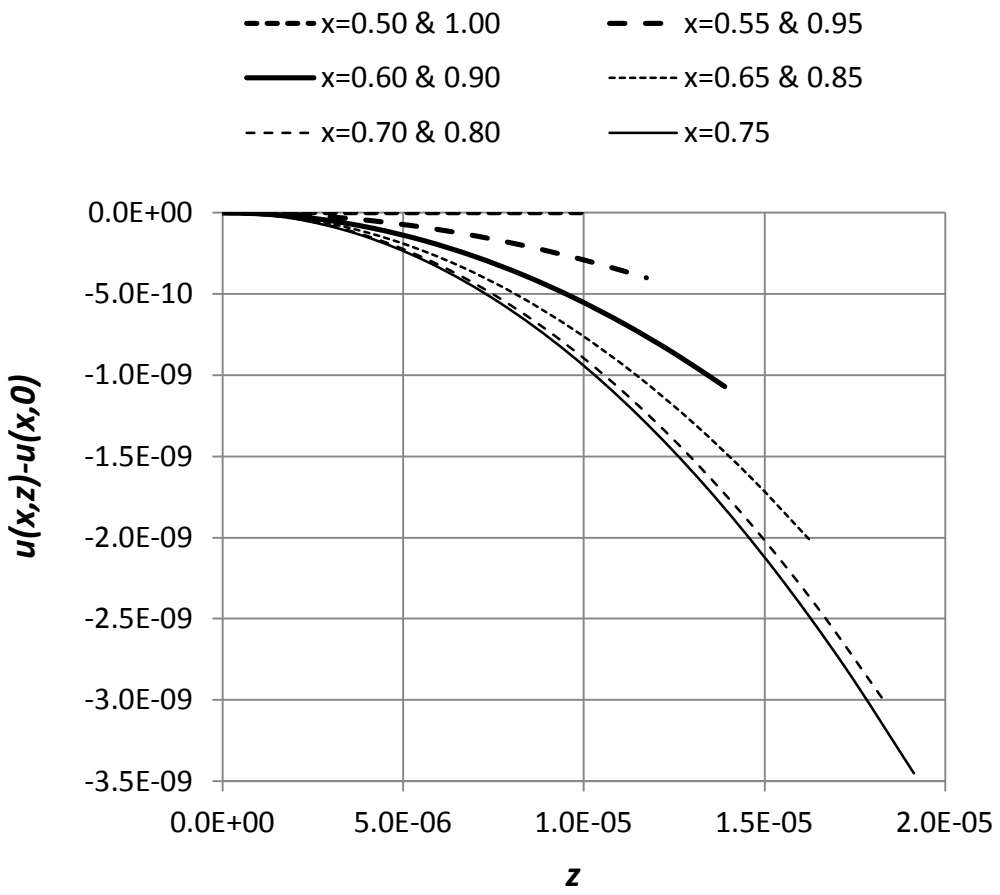

Fig 11 *u(x, z)-u(x, 0)* for x = 0.50, 0.55, 0.60, 0.65, 0.70, 0.75, 0.80, 0.85, 0.90, 0.95, 1.00 with L = 1 E - 5, V = 3 E - 5

Figure 12 is a graph of the dimensionless transverse specific discharge *w* at the upper wall and at specified fractions of the channel half width. This demonstrates that the flow moves toward or away from the centerplane in phase with the wall, but with an amplitude that decreases to zero as the centerplane is approached.

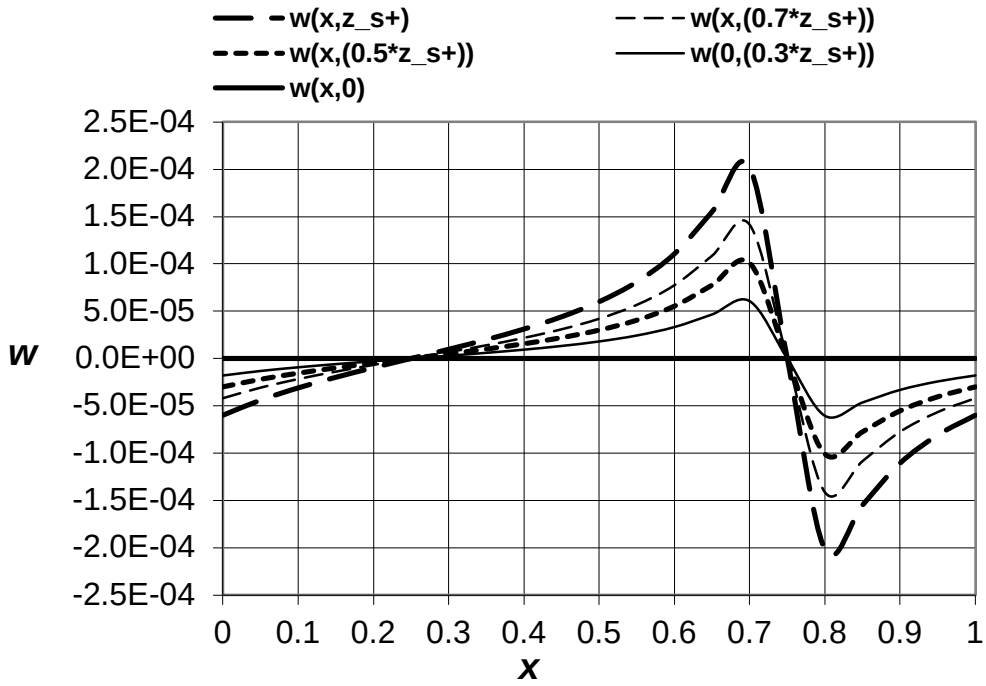

Fig. 12 Dimensionless transverse specific discharge *w* at specified fractions of the channel half width as a function of *x* for $L = 1\ \mathrm{E} - 5$ and $\mathcal{V} = 6\ \mathrm{E} - 5$.

4 Conclusions

This paper presents an analytical solution for the steady flow of an incompressible fluid through a homogeneous, isotropic porous medium filling a channel bounded by symmetric wavy walls. The channel walls change from parallel planes, to small amplitude sine waves, to large amplitude nonsinusoidal waves as certain parameters are increased. The direction of gravity is arbitrary. A plot of piezometric head against distance in the direction of mean flow changes from a straight line for parallel planes to a series of steeply sloping sections in the reaches of small aperture and high specific discharge alternating with nearly constant sections in the large aperture, low specific discharge bulges. Expressions are

given for the stream function, specific discharge, piezometric head, and pressure. These conclusions can be useful in investigating the effect of velocity variations along a fracture on reactive transport properties of the fracture due to migration of CO_2-saturated brine in a carbon storage application.

Acknowledgements This technical effort was performed in support of the National Energy Technology Laboratory's ongoing research in CO_2 capture under the RES contract DE-FE0004000.

References

Auriault, J-L.: On the domain of validity of Brinkman's equation, Transp Porous Med 79, 215-223 (2009)

Bear, J.: Dynamics of Fluids in Porous Media, Elsevier, New York, 129-132 and 222-226 (1972)

Chow, J.C.F., Soda, K., Dean, C.: On laminar flow in wavy channels. In Developments in Mechanics, Vol. 8, Proceedings of the 12th Midwestern Mechanics Conference, 247-260, University of Notre Dame Press, Notre Dame, Indiana (1971)

Crandall, D., Bromhal, G., Karpyn, Z.T.: Numerical simulations examining the relationship between wall-roughness and fluid flow in rock fractures, International Journal of Rock Mechanics and Mining Sciences 47, 5, 784-796 (2010)

Datta, S., Tripathi, A.: Study of steady viscous flow through a wavy channel: non-orthogonal coordinates, Meccanica 45, 809-815 (2010)

Domenico, P.A., Schwartz, F.W.: Physical and Chemical Hydrogeology 2nd ed., Wiley, New York, 50-51 (1998)

Hughes R.G., Blunt, M.J.: Network modeling of multiphase flow in fractures, Adv. Water Resources 24, 409–21 (2001)

Huitt, J.L.: Fluid flow in simulated fractures, AIChE J 2, 259-264 (1956)

Konzuk J.S., Kueper, B.H.: Evaluation of cubic law based models describing single-phase flow through a rough-walled fracture, Water Resources Research 40 (2004) W02402, DOI:10.1029/2003WR002356

Ng, C.-O., Wang, C.Y.: Darcy-Brinkman flow through a corrugated channel, Transp Porous Med 85, 605-618 (2010)

Nishimura, T., Ohori, Y., Kawamura, Y.: Flow characteristics in a channel with symmetric wavy wall for steady flow, J Chem Eng Japan 17, 466-471 (1984)

Piri M., Karpyn, Z.T.: Prediction of fluid occupancy in fractures using network modeling and X-ray microtomography. II: Results, Phys Rev E 76, 016316 (2007) DOI:10.1103/PhysRevE.76.016316, 11 pages

Romm, E.S.: Flow Characteristics of Fractured Rocks (in Russian), Nedra, Moscow (1966)

Zimmerman, R.W., Bodvarsson, G.S.: Hydraulic conductivity of rock fractures, Transp Porous Med 23, 1-30 (1996)